LAWRENCE
LIVERMORE
NATIONAL
LABORATORY

LLNL-PROC-405519

An Experimental Investigation of Structural Effects on the Auto-Ignition Properties of Two C5 Esters

S. M. Walton, M. S. Wooldridge, C. Westbrook

July 18, 2008

32nd International Symposium on Combustion
Montreal, Canada
August 3, 2008 through August 8, 2008

Disclaimer

An Experimental Investigation of Structural Effects on the Auto-Ignition Properties of Two C_5 Esters

S. M. Walton[*,a], M. S. Wooldridge[a], and C. K. Westbrook[b]

[a] *Department of Mechanical Engineering, University of Michigan, 2350 Hayward St., Ann Arbor, Michigan 48109*

[b] *Lawrence Livermore National Laboratory, Livermore, California 94550*

[*] *Corresponding author.* E-mail address: smwalton@umich.edu

Abstract

Ignition studies of two C_5 esters were performed using a rapid compression facility. Methyl butanoate and ethyl propanoate were chosen to have matching molecular weights and C:H:O ratios while varying the length of the constituent alkyl chains. The effect of functional group size on ignition delay time was investigated using pressure time-histories and high-speed digital imaging. Low-temperature, moderate-pressure conditions were selected for study due to the relevance to low temperature combustion strategies and internal combustion engine conditions. The experiments covered a range of conditions: T=935-1117 K, P=4.7-19.6 atm, and ϕ=0.3-0.4. The experimental data are compared to previous high temperature studies and chemical modeling. A new mechanism for methyl butanoate and ethyl propanoate ignition is presented. The modeling and experimental data are in excellent agreement for methyl butanaote and yield good agreement for ethyl propanoate.

Keywords: Biofuel; Ester; Ignition; Rapid Compression Facility; Chemical Reaction Mechanism

1. Introduction

With the large scale efforts proposed to replace petroleum-derived fuels with biofuels come many challenges, as well as opportunities. The positive renewable attributes of biofuels can be combined with advanced combustion strategies to increase thermodynamic efficiencies and to lower some pollutant emissions. Challenges associated with biorenewable fuels include increased production of oxygenated pollutant compounds, such as aldehydes and other harmful carbonyls including ozone precursors; erratic performance characteristics due to variability in the fuel properties as a function of the feedstock material and fuel processing; and degradation of the fuel during distribution and storage.

Successful implementation of biorenewables into the fuel infrastructure requires a predictive understanding of the impact of the biofuels on combustion performance and emissions. A critical component to achieving this goal is a fundamental understanding of the effects of oxygenated hydrocarbon (OHC) structure on combustion chemistry. This is particularly necessary as modern engine design moves towards low-temperature strategies which become kinetically controlled by slower, complex low-temperature chemistry. Recent studies have attempted to address the deficiency in the literature on quantitative understanding of the reaction chemistry of esters and other OHCs (e.g. methyl butanoate [1–3], ethyl propanoate [4], additional $C_5H_{10}O_2$ ester isomers [5], dimethyl ether [6], dimethyl carbonate [7], butyl alcohols [8], methyl acetate [9], ethyl acetate [10], ethyl formate [9], and alkyl ethers [11] to name a few). However, there are still few data which isolate the effects of structure on reaction chemistry, particularly at pressures and temperatures of interest to modern engine and combustor design.

This work is part of a larger effort to develop the reference data and tools necessary to understand and predict the effects of OHC structure on the combustion properties of real biofuels. The objective of this work is to quantify the effects of changes in fuel structure on the ignition properties of two representative C_5 esters: methyl butanoate (CCC(C=O)OC) and ethyl propanoate (CC(C=O)OCC). Both experimental and reaction modeling approaches were used. The experimental effort focused on evaluating the ignition delay time of the two esters over a range of pressures, temperatures and mixture compositions using a rapid compression facility (RCF). The modeling effort focused on modifying the reaction chemistry of existing mechanisms for methyl butanoate and ethyl propanoate to accommodate the low-temperature conditions studied in this work.

2. Experimental Approach

The University of Michigan (UM) RCF is a unique experimental apparatus, capable of creating uniform high temperature (T=500-3000 K) and high pressure (P=0.5-60 atm) conditions [12] that are directly applicable to many

practical combustion devices, including diesel and homogeneous charge compression ignition engines. The ignition delay time (τ_{ign}), an important chemical kinetic characteristic of reference combustion compounds, can be determined from UM RCF experiments using pressure time-histories and digital imaging.

A detailed description of the UM RCF, detailed schematics, the operating procedure, and the results of benchmark experimental studies characterizing performance have been presented previously [12, 13]. Briefly, the UM RCF consists of five major components: the driver section, the driven section, the test manifold, the sabot (free piston), and the hydraulic control valve assembly. Prior to each experiment, the driven section is evacuated with a diffusion pump, and the driver section is filled with high pressure air, with the sabot located at the upstream end of the driven section. The driver section and the driven section are separated by the hydraulic control valve assembly, and a scored sheet of plastic (0.5 mm thick, Mylar®). After filling the driven section with a previously prepared test gas mixture, the hydraulic globe valve is opened, allowing the high pressure air to break the plastic sheet, and rapidly accelerate the sabot. The test gas mixture is compressed in front of the sabot, and when the nosecone seats (by an annular interference fit with the test manifold walls) the test gases are sealed into the test section. A schematic of the test manifold is shown in Fig. 1. The four main components of the test manifold are the convergent section, the extension section, the instrumented test section, and a transparent end wall. The stainless steel convergent section bridges the 101.2 mm bore of the driven section to the 50.8 mm bore of the remainder of the test manifold components. The total length of the extension section is variable by design to yield different compression ratios (shown as CR≅26 in Fig. 1), and was varied from ∼23-29 for the data set presented here. For the current study, the UM RCF was instrumented with a piezoelectric transducer (Kistler 6041AX4) and charge amplifier (Kistler 5010B) for pressure measurements in the test volume, and an uncoated polycarbonate end wall was used to provide end view optical access to the entire test manifold.

Images were acquired using a high-speed color digital video camera (Vision Research, Phantom V7.1) at 26,000 frames per second (fps). A fast 50 mm lens (f/0.95 Navitar) and c-mount extension tube were used with the camera to optimize the capture of visible light emission. A more detailed description of the imaging setup and procedure can be found in Walton *et al.* [14].

3. Results and Discussion

3.1. Experimental Data

Mixtures and conditions for study were selected to compare the ignition properties of the two $C_5H_{10}O_2$ isomers: methyl butanoate and ethyl propanoate. Specifically, the temperature varied from T=935-1117 K, the pressure varied

from P=4.7-19.6 atm, and lean conditions were studied (ϕ=0.3-0.4). The dilution of the fuel and O_2 mixtures was kept constant throughout this study with (total inert gases)/$O_2 \cong 3.76$. The inert gases were varied (Ar, N_2, or CO_2) to assist in controlling the end of compression pressure and temperature.

Typical pressure and pressure derivative data for $C_5H_{10}O_2$ ignition experiments are shown in Fig. 2. The initial pressure rise is due to compression of the test gas mixture ahead of the sabot. At the end of compression, the pressure reaches the first maximum. This time is set as t = 0 sec and is labeled P_{max} in the figure. The pressure then decreases slightly due to cooling losses to the test volume walls. After a delay period, the mixture auto-ignites resulting in a rapid increase in pressure for all cases. As demonstrated in Fig. 2, none of the experimental data presented in this study exhibited two-stage ignition behavior.

The effective test conditions were determined using the pressure time-history from each experiment. The effective pressure (P_{eff}) was defined as the time-averaged pressure from the maximum pressure (P_{max}) at the end of compression to the point of maximum rate of pressure rise (dP/dt_{max}), or

$$P_{eff} = \frac{1}{(t_{dP/dt_{max}} - t_{P_{max}})} \times \int_{t_{P_{max}}}^{t_{dP/dt_{max}}} P \cdot dt. \tag{1}$$

The effective temperature (T_{eff}) for each experiment was determined, as in previous UM RCF studies [12–14], using the effective pressure and by numerical integration of the isentropic relation

$$\int_{T_o}^{T_{eff}} \frac{\gamma}{\gamma - 1} \, d\, ln(T) = ln\left(\frac{P_{eff}}{P_o}\right), \tag{2}$$

where P_o is the initial charge pressure, T_o is the initial temperature (typically 298 K), and γ is the temperature-dependent ratio of the specific heats of the unreacted test gas mixture, which is determined using the NASA thermodynamic data base [15].

For each experiment, the ignition delay time (τ_{ign}) was determined using the pressure time-history, and defined as the time between P_{max} and dP/dt_{max}. This definition for τ_{ign} is illustrated in Fig. 2, and was developed in previous UM RCF ignition studies [14]. This definition is very robust when different ignition regimes are present.

High speed imaging was also acquired for each ignition experiment. The imaging was used to ensure the homogeneity of the ignition conditions in the test volume for each experiment. An imaging sequence corresponding to the pressure time-history for methyl butanoate ignition is shown in Fig. 3. As seen in Fig. 3, the mixture ignites uniformly with little spatially resolved structure. The peak in the blue emission corresponds to the maximum in the

pressure derivative. Note the pressure remains approximately constant during the ignition delay. Similar ignition behavior was observed for the ethyl propanoate experiments. A typical pressure time-history for ethyl propanoate is included in Fig. 2. The general features of the pressure data are similar for both esters. The imaging data (not included here for ethyl propanoate) demonstrate uniform volumetric ignition. An uncertainty analysis was completed using the same method described in He *et al.* [13] and Walton *et al.* [14]. The average uncertainty for the τ_{ign} measurements for this study is $\pm 16\%$ for both methyl butanoate and ethyl propanoate, and is primarily due to the uncertainty in the pressure measurement.

A summary of the methyl butanoate ignition data, including the measured ignition delay time and test conditions for each experiment, is presented in Table 1. Table 2 presents a summary of the ethyl propanoate results. Figure 4 provides a summary of the results for τ_{ign} for both esters studied in this work for P$\cong$10 atm. The data are compared with previous high-temperature studies of $C_5H_{10}O_2$ ester ignition. The data from Metcalfe *et al.* [4] were obtained at lower pressures (P = 1 and 4 atm), and over the temperature range T=1100-1670 K, with ϕ=1.0. Metcalfe *et al.* [4] refined the mechanism for methyl butanoate oxidation of Fisher *et al.* [2] to include ethyl propanoate and to obtain better agreement at the conditions they investigated. The results of their model predictions are shown in Fig. 4. As seen in Fig. 4 for methyl butanoate, the low temperature results from the present experiments show a smaller effective activation energy than the high temperature results of Metcalfe *et al.* [4]. In addition, the low temperature ethyl propanoate ignition data indicate a higher effective activation energy than the low temperature data for methyl butanoate. Insight into these differences can be gained through detailed kinetic modeling, which can also be used to reconcile the apparently different high and low temperature trends.

Overall, the experimental results show that ethyl propanoate ignites more rapidly than methyl butanoate under the same experimental conditions. This is consistent with analyses by Schwartz *et al.* [5] and Metcalfe *et al.* [4], who showed that the two isomers react via quite different reaction pathways. Methyl butanoate reacts primarily through bimolecular reactions in which radical species abstract H atoms from methyl butanoate; the resulting radical species from methyl butanoate then decompose and produce additional radical species to continue the process. In contrast, ethyl propanoate reacts via a much different pathway, with a particularly low energy barrier that is not available to methyl butanoate. This pathway involves the formation of a six-membered transition state that transfers an H atom from the ethyl group in ethyl propanoate to the C=O group within the molecule. This transition state then decomposes rapidly to produce ethene and propanoic acid, both of which are much more reactive than methyl butanoate. This reaction pathway is not possible for methyl butanoate, since its methyl group enables only a five-membered transition state that has a much higher activation energy barrier for H atom transfer. The same

six-membered transition state, producing ethene and a carboxylic acid, is important in oxidation of ethyl formate and ethyl acetate [16], and the same rate expression is used in the present ethyl propanoate reaction mechanism [4].

Metcalfe *et al.* [4] considered the possible formation of an intermediate ring during methyl butanoate decomposition. They added this reaction step to their modified reaction mechanism, and modeled the ring as forming from the carbonyl group, and the C atoms in the alkyl chain of the acid group. However, they found that this pathway contributes very little ($<1\%$) to the methyl butanoate decomposition for the conditions they studied.

The UM RCF results are consistent with the trends observed in the high-temperature studies by Schwartz *et al.* [5] and Metcalfe *et al.* [4]. As such, we propose that ethyl propanoate favors the more rapid reaction sequence of unimolecular decomposition at these low-temperature conditions as well. Additional experimental measurements of the key intermediates can help quantify the relative contributions of the decomposition reactions and clarify the overall reaction sequence.

3.2. Kinetic Modeling

Metcalfe *et al.* [4] recently added an ethyl propanoate submechanism to the methyl butanoate mechanism of Fisher *et al.* [2] and included a few revised reaction rates (including H atom abstraction from methyl butanoate and formaldehyde production) from Gaïl *et al.* [3]. In the current work, the reaction mechanism from Metcalfe *et al.* [4] was modified slightly to improve the agreement between the computed and experimental results. For the conditions of this experimental study, H atom abstraction from the C_5 ester by HO_2 accelerates ignition by forming H_2O_2, which then decomposes into two OH radicals. H abstraction from the C_5 ester by H atoms decreases the overall rate of ignition because these reactions compete with the principal chain branching reaction between H and O_2, producing O and OH radicals. Since the computed results were uniformly more reactive than the experiments, the A-coefficients for the two most sensitive reactions between methyl butanoate and H were increased by a factor of two (mb+h=h2+mb4j, mb+h=h2+mbmj), and the remaining mb + H reactions were changed to the generalized Arrhenius form to span the temperature range of both the UM RCF data and the Metcalfe *et al.* [4] shock tube data. Additionally, the A-coefficients for all of the reactions between methyl butanoate and HO_2 were decreased by a factor of 0.77, and the A-coefficients for all of the forward reactions between ethyl propanoate and HO_2 were decreased by a factor of 0.65. The specific reactions and the modified rate coefficient expressions are summarized in Table 3. Note these small changes are within the uncertainty bounds for each of the reaction rate expressions.

All of the simulations of the UM RCF experiments assumed that combustion takes place homogeneously at constant volume, with negligible heat loss during the ignition delay period. No reaction was considered during the compression stroke, which is appropriate unless the ignition delay becomes very short compared with the last few

milliseconds of the compression stroke. Ignition was defined computationally as the maximum rate of temperature rise of the reacting mixture.

Computed results from the modified mechanism for methyl butanoate ignition are shown as the solid and dashed lines in Fig. 5, calculated for ϕ = 0.4 and 0.3, respectively, and at 10 atm pressure. The UM RCF results for both ϕ = 0.3 and 0.4 are shown as symbols. The experimental results include the ϕ=0.3 and 0.4 cases for pressures between 7.9 and 14.7 atm. Model predictions for the experimental conditions that extend beyond P=10 atm are shown in Table 1. The overall agreement between the computed and experimental results is excellent at both low and high-temperatures. The computed curve extends to high temperatures, showing a perceptible increase in the overall slope or effective activation energy. Computed results for methyl butanoate ignition at ϕ = 1 and 4 atm are shown as the dotted curve, indicating the predicted change in ignition delay that should be expected for the difference due to the larger equivalence ratio and lower pressure between the two experimental studies.

Computed results for ethyl propanoate are shown as the solid and dashed lines in Fig. 6, calculated for ϕ = 0.4 and 0.3, respectively, and at 10 atm pressure. The UM RCF results for both ϕ = 0.3 and 0.4 are also shown. The two curves show the expected changes in ignition delay time as the equivalence ratio is changed from 0.4 to 0.3 at fixed pressure. Some of the experimental results agree very well with the modeling results, while others are slower than the calculated values by a factor of about 2. The Metcalfe *et al.* [4] high-temperature shock tube results are shown in Fig. 6, describing experiments at ϕ = 0.25 and 0.5, both at 4 atm pressure. Modeling results for the Metcalfe *et al.* mixtures at ϕ = 0.5 are shown as the dotted curve in Fig. 6.

The results for methyl butanoate and ethyl propanoate both show the same curvature in the computed ignition delay curves between 1100 K and 1200 K, producing a somewhat lower effective activation energy at lower temperatures. The modeling calculations show that this effect is due to the emergence of H atom abstraction reactions from these fuels by HO_2 and CH_3O_2 radicals as temperature decreases, which produce H_2O_2 and CH_3O_2H respectively. At these temperatures, these products rapidly decompose to yield OH + OH and CH_3O + OH, providing chain branching and a more rapid ignition. However, none of the reaction temperatures are low enough to determine whether or not alkylperoxy radical isomerization reaction and a negative temperature coefficient (NTC) region should be expected for these fuels. Based on the length of the hydrocarbon chains in both molecules, such NTC behavior is quite unlikely, in agreement with comments by Gaïl *et al.* [3]. The computations agree with the experimental results that methyl butanoate is slower to ignite than the other fuels and that part of the difference is related to the fact that the six-centered molecular elimination reaction of methyl butanoate is slower and leads to less reactive intermediate species than the corresponding reactions in ethyl propanoate.

We have used the kinetic modeling results to connect the high temperature ignition results of Metcalfe *et al.* [4] and the present intermediate temperature ignition experiments into a single, internally consistent family of ignition results, which assists in the extraction of analytical results from the experiments. For example, use of the experimental RCF results alone for ethyl propanoate would suggest an effective activation energy of 45.6 kcal/mol, although the slope of the curve in Fig. 6 shows that this value should be closer to 31 kcal/mol. Alternatively, extrapolation of the high-temperature activation energy for methyl butanoate to low temperatures would lead to a significant error.

4. Summary and Conclusions

This work presents the first rapid compression facility data on low temperature ignition of methyl butanoate and ethyl propanoate. The UM RCF data indicate a lower activation energy for methyl butanoate over the temperature range (T=935-1109 K) considered here, when compared to the higher temperature ignition data in the existing literature. Ethyl propanoate exhibited faster ignition delay times compared to methyl butanoate for the ϕ=0.3-0.4 conditions studied. The results support the supposition that methyl butanoate consumption is dominated by relatively slow bimolecular H-atom abstraction reactions, whereas ethyl propanoate consumption is dominated by faster unimolecular decomposition. Ester molecular structure is not only important for identifying and quantifying ignition properties; Schwartz *et al.* [5] have suggested that the formation of an intermediate ring structure can lead to the formation of aromatics and soot through the formation of highly reactive alkenes, such as propene and the subsequent formation of propargyl radicals. The majority of biodiesels are comprised primarily of methyl and ethyl esters. The actual chemical composition is a function of plant feedstock as well as processing method, fuel age, etc. Understanding the differences in decomposition pathways for esters of different structure is necessary to develop predictive rules for how different biodiesels will react. The present work is part of a longer-term effort to understand the chemistry and combustion properties of biofuels in general. This study presents ignition behavior of key reference compounds that exhibit features we expect will remain important for real biofuels. Further studies of ester intermediates can help clarify and quantify these important reaction sequences.

Acknowledgments

The authors would like to acknowledge the generous support of the Department of Energy through the University of Michigan HCCI Consortium. Prepared by LLNL under Contract DE-AC52-07NA27344.

References

[1] C. K. Westbrook, W. J. Pitz, and H. J. Curran. *J. Phys. Chem. A*, 110(21):6912–6922, 2006.

[2] E. M. Fisher, W. J. Pitz, H. J. Curran, and C. K. Westbrook. *Proc. Combust. Inst.*, 28(2):1579–1586, 2000.

[3] S. Gaïl, M. J. Thomson, S. M. Sarathy, S. A. Syed, P. Dagaut, P. Divart, A. J. Marchese, and F. L. Dryer. *Proc. Combust. Inst.*, 31(1):305–311, 2007.

[4] W. K. Metcalfe, S. Dooley, H. J. Curran, J. M. Simmie, A. M. El-Nahas, and M. V. Navarro. *J. Phys. Chem. A*, 111(19): 4001–4014, 2007.

[5] W. R. Schwartz, C. S. McEnally, and L. D. Pfefferle. *J. Phys. Chem. A*, 110(21):6643–6648, 2006.

[6] X. L. Zheng, T. F. Lu, C. K. Law, C. K. Westbrook, and H. J. Curran. *Proc. Combust. Inst.*, 30(1):1101–1109, 2005.

[7] P. A. Glaude, W. J. Pitz, and M. J. Thomson. *Proc. Combust. Inst.*, 30(1):1111–1118, 2005.

[8] C. S. McEnally and L. D. Pfefferle. *Proc. Combust. Inst.*, 30(1):1363–1370, 2005.

[9] P. Osswald, U. Struckmeier, T. Kasper, K. Kohse-Hoinghaus, J. Wang, T. A. Cool, N. Hansen, and P. R. Westmoreland. *J. Phys. Chem. A*, 111(19):4093–4101, 2007.

[10] L. Gasnot, V. Decottignies, and J. F. Pauwels. *Fuel*, 84(5):505–518, 3 2005.

[11] C. S. McEnally and L. D. Pfefferle. *Int. J. Chem. Kinet.*, 36(6):345–358, 2004.

[12] M. T. Donovan, X. He, B. T. Zigler, T. R. Palmer, M. S. Wooldridge, and A. Atreya. *Combust. Flame*, 137(3):351–365, 2004.

[13] X. He, M. T. Donovan, B. T. Zigler, T. R. Palmer, S. M. Walton, M. S. Wooldridge, and A. Atreya. *Combust. Flame*, 142: 266–275, 2005.

[14] S. M. Walton, X. He, B. T. Zigler, M. S. Wooldridge, and A. Atreya. *Combust. Flame*, 150:246–262, 2007.

[15] B. J. McBride, S. Gordon, and M. A. Reno. Nasa thermodynamic data base. *NASA Technical Memorandum 4513*, 1993.

[16] C. K. Westbrook, W. J. Pitz, P. R. Westmoreland, F. L. Dryer, M. Chaos, P. Osswald, K. Kohse-Hoinghaus, T. A. Cool, J. Wang, B. Yang, H. Hansen, and T. Kasper. *Submitted to Proc. Combust. Inst.*, 32, 2008.

Table 1: Summary of experimental conditions and results, and modeling results for methyl butanoate ignition. All mixture composition data are provided on a mole basis. The equivalence ratio (ϕ) is based on the C to O molar ratios of the actual and stoichiometric conditions. The inert gas to O_2 molar ratio $\cong$ 3.76 for all experiments. Model predictions for ignition delay times were made using the modified methyl butanoate/ethyl propanoate reaction mechanism and are listed as τ_{pred}.

ϕ	Test gas composition[a]				P_{eff} [atm]	T_{eff} [K]	τ_{ign} [ms]	τ_{pred} [ms]
	χ_{mb} [%]	χ_{O_2} [%]	χ_{N_2} [%]	χ_{Ar} [%]				
0.40	1.27	20.8	74.7	3.3	9.8	938	33	30
0.40	1.27	20.8	74.7	3.3	9.6	935	37	32
0.40	1.27	20.8	62.3	15.7	9.9	992	15	13
0.40	1.27	20.7	51.7	26.3	10.3	1053	6.3	6.8
0.40	1.27	20.8	42.3	35.7	10.5	1109	2.7	4.2
0.38	1.20	20.8	62.4	15.6	5.4	1015	22	21
0.39	1.24	20.8	62.5	15.4	4.9	989	37	30
0.39	1.26	20.7	62.4	15.6	5.4	1014	18	20
0.40	1.28	20.7	74.7	3.3	10.4	953	24	22
0.40	1.27	20.7	74.7	3.3	11.1	969	17	17
0.30	0.95	20.8	68.7	9.5	10.2	998	16	15
0.30	0.95	20.8	68.7	9.5	10.4	1005	14	14
0.30	0.96	20.7	68.5	9.6	14.7	991	11	12
0.30	0.96	20.8	68.6	9.6	14.5	988	12	13
0.30	0.96	20.8	68.6	9.5	18.6	978	9.8	11
0.30	0.96	20.8	68.6	9.6	19.6	991	7.7	9.1
0.30	0.96	20.8	68.7	9.6	5.0	994	47	33
0.30	0.96	20.8	68.7	9.6	4.7	979	49	43
0.30	0.95	20.8	61.1	17.2	7.9	1046	10	12
0.30	0.95	20.8	61.1	17.2	7.9	1047	11	12
0.30	0.95	20.8	52.5	25.7	8.1	1094	4.7	7.2
0.30	0.96	20.8	52.4	25.9	8.1	1098	4.6	6.9

[a]Balance CO_2

Table 2: Summary of experimental conditions and results, and modeling results for ethyl propanoate ignition. All mixture composition data are provided on a mole basis. The equivalence ratio (ϕ) is based on the C to O molar ratios of the actual and stoichiometric conditions. The inert gas to O_2 molar ratio $\cong$ 3.76 for all experiments. Model predictions for ignition delay times were made using the modified methyl butanoate/ethyl propanoate reaction mechanism and are listed as τ_{pred}.

	Test gas composition[a]				P_{eff}	T_{eff}	τ_{ign}	τ_{pred}
ϕ	χ_{ep} [%]	χ_{O_2} [%]	χ_{N_2} [%]	χ_{Ar} [%]	[atm]	[K]	[ms]	[ms]
0.40	1.27	20.7	51.6	26.4	10.6	1064	2.9	3.3
0.40	1.27	20.7	51.6	26.4	10.6	1064	2.8	3.3
0.30	0.96	20.8	68.7	9.5	9.6	988	20	14
0.30	0.96	20.8	68.7	9.5	9.8	995	17	12
0.30	0.96	20.8	58.1	20.2	10.5	1061	5.9	4.0
0.30	0.96	20.8	58.0	20.2	10.8	1068	5.2	3.6
0.30	0.96	20.8	48.7	29.5	10.7	1117	1.4	1.7
0.30	0.96	20.8	48.7	29.5	10.4	1109	1.5	2.0

[a]Balance CO_2

Table 3: Summary of reactions[a] modified in this work for the methyl butanoate/ethyl propanoate reaction mechanism. The remainder of the mechanism was unchanged from Metcalfe *et al.* [4]. The rate coefficients are listed in the generalized Arrhenius form $k = AT^n exp(-E_a/RT)$[b]

Reaction	A	n	E_a
mb + ho2 = h2o2 + mb4j	1.900×10^{12}	0.0	20440
mb + ho2 = h2o2 + mb3j	1.300×10^{12}	0.0	17690
mb + ho2 = h2o2 + mb2j	1.300×10^{12}	0.0	17690
mb + ho2 = h2o2 + mbmj	1.900×10^{12}	0.0	20440
mb + h = h2 + mb4j	1.880×10^{5}	2.75	6280
mb + h = h2 + mb3j	1.300×10^{6}	2.4	4471
mb + h = h2 + mb2j	1.300×10^{6}	2.4	4471
mb + h = h2 + mbmj	1.880×10^{5}	2.75	6280
ep + ho2 = h2o2 + ep3j	8.300×10^{3}	2.55	16490
ep + ho2 = h2o2 + ep2j	1.500×10^{12}	0.0	14400
ep + ho2 = h2o2 + epej	2.500×10^{3}	2.55	10530
ep + ho2 = h2o2 + epmj	8.300×10^{3}	2.55	16490

[a]Notation from Metcalfe *et al.* [4]

[b]Units are mole, cm, sec., cal., and K

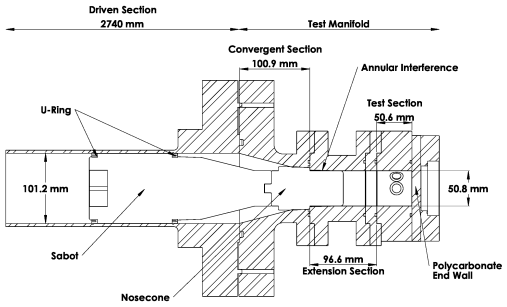

Fig. 1: Experimental schematic of the test section of the UM RCF. The sabot nosecone is shown in the final seated position.

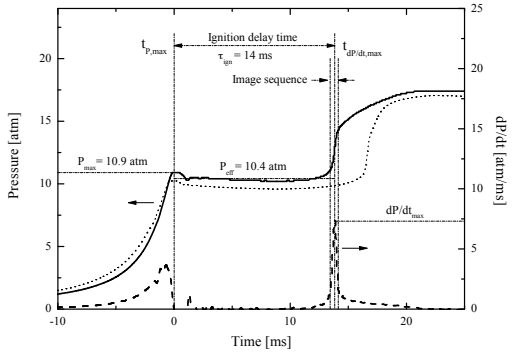

Fig. 2: Typical pressure (——) and pressure derivative (- - -) time-histories for methyl butanoate ignition experiments with experimental conditions; P_{eff}=10.4 atm, T_{eff}=1005 K, ϕ=0.30, Inert/O_2=3.76, τ_{ign}=14 ms. Also included in this figure are typical pressure time-history data for ethyl propanoate; (· · ·, P_{eff}=9.8 atm, T_{eff}=995 K, ϕ=0.30, Inert/O_2=3.76, τ_{ign}=17 ms).

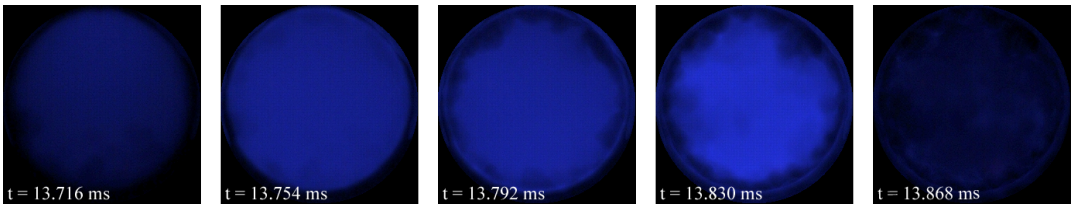

Fig. 3: Imaging sequence corresponding to the methyl butanoate data and time interval presented in Fig. 2 (26,000 fps, color adjusted for clarity).

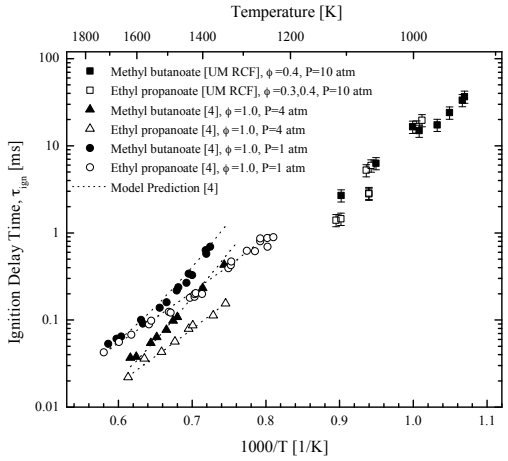

Fig. 4: Comparison of current ($P_{eff} \cong$10 atm data) and previous ignition delay time studies for $C_5H_{10}O_2$ isomers. The high temperature data are from Metcalfe *et al.* [4], and the dotted lines ($\cdot\ \cdot\ \cdot$) are their associated model predictions. The error bars represent the uncertainty in the UM RCF data.

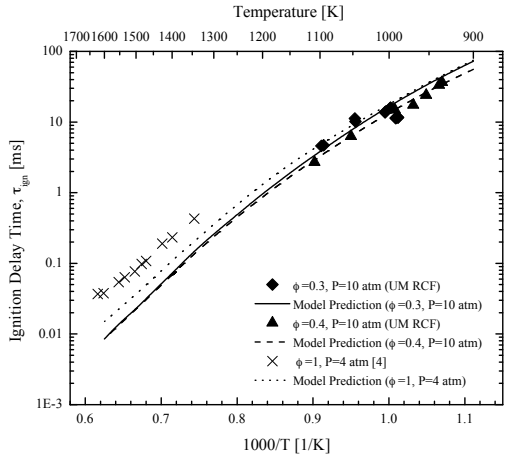

Fig. 5: Comparison of model predictions with current and previous experimental data for methyl butanoate ignition. The solid (——) line is the model prediction for the ϕ=0.3, low temperature conditions of this study. The dashed (- - -) line is the model prediction for the ϕ=0.4, low temperature conditions of this study. The dotted ($\cdot\ \cdot\ \cdot$) line is the model prediction for the high temperature, stoichiometric conditions of Metcalfe *et al.* [4].

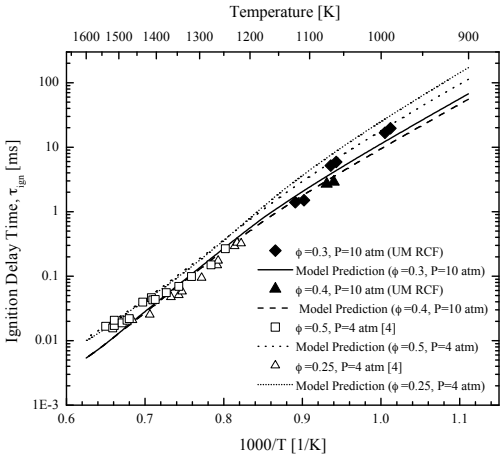

Fig. 6: Comparison of model predictions with current and previous experimental data for ethyl propanoate ignition. The solid (——) line is the model prediction for the ϕ=0.3, low temperature conditions of this study. The dashed (- - -) line is the model prediction for the ϕ=0.4, low temperature conditions of this study. The dotted ($\cdot\ \cdot\ \cdot$) line is the model prediction for the ϕ=0.5, high temperature conditions of Metcalfe *et al.* [4]. The short dotted ($\cdot\ \cdot\ \cdot$) line is the model prediction for the ϕ=0.25, high temperature conditions of Metcalfe *et al.* [4].

5. *

List of Tables

6. *

List of Figures